A PRINTED CIRCUIT HYBRID-RING DIRECTIONAL COUPLER FOR ARBITRARY POWER DIVISIONS

Ashok K. Agrawal and Gerald F. Mikucki

RCA Missile and Surface Radar Division
Moorestown, NJ 08057

ABSTRACT

A directional coupler in the form of a hybrid ring particularly suited for printed circuits is described. The maximum power-split ratio between the two output ports of a printed- circuit conventional hybrid ring coupler is limited by the highest impedance line that can be realized [1]. The hybrid-ring directional coupler described in this paper allows a larger power-split ratio for the same impedance lines, and thereby increases the range of the power-split ratio that can be realized for printed circuits. A theoretical analysis was conducted using the scattering matrix, and experimental verification of the theoretical results was achieved in a stripline configuration at Ku-band.

INTRODUCTION

In printed circuit array antennas, the hybrid-ring directional coupler is an appealing choice for the basic power division element in beamforming networks for two primary reasons: (a) the output arms are isolated from each other, and (b) the input impedance is matched when the remaining arms are terminated by matched impedances. Since the conventional T (or Y) junction power dividers do not possess these properties, directional couplers are preferable for antenna array feed systems where the isolation between the output arms of the power divider is essential in order to minimize mutual coupling between radiating elements.

The configuration of a conventional hybrid-ring directional coupler is shown in Figure 1. The characteristic admittances of the four arms are normalized to unity. The variable parameters Y_1 and Y_2 represent the characteristic admittances of two lines of the ring. They determine the degree of coupling of the output arms and the matching condition for the input arm. When the signal is fed into sum port 3, the output voltages in arms 1 and 2 are in phase, and their relative amplitudes are related by

$$\frac{b_1}{b_2} = \frac{Y_2}{Y_1} \qquad [1]$$

When the signal is fed into difference port 1, the output voltages in arms 3 and 4 are 180° out-of-phase, and their relative amplitudes are related by

$$\frac{b_3}{b_4} = -\frac{Y_2}{Y_1} \qquad [2]$$

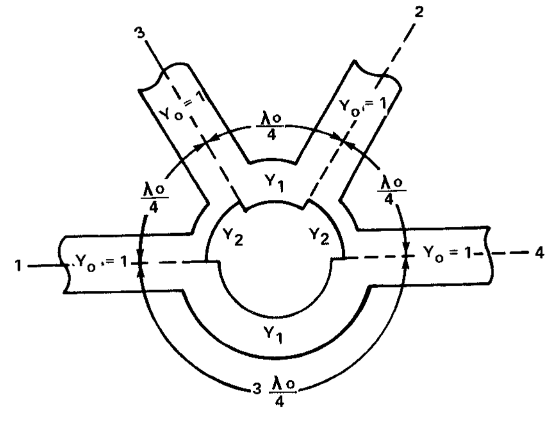

Fig. 1 Conventional hybrid-ring directional coupler.

In both cases, the condition that the input arm be perfectly matched requires that Y_1 and Y_2 satisfy the condition

$$Y_1^2 + Y_2^2 = 1 \qquad [3]$$

From equations [1] and [2], it is evident that the output voltage ratio is directly proportional to the ratio of the characteristic admittances (or impedances) of the transmission lines forming the ring. The impedance values required for various power-split ratios are presented in Table 1. In microstrip and stripline circuits, the highest impedance line that can be realized limits the maximum power-split ratio between the two output arms. The highest attainable impedance value for striplines and microstrips is a function of the physical characteristics of the substrate (e.g., dielectric constant and thickness). The practical impedance limit for most substrates, using conventional etching techniques, is around 150 ohms. Referring to Table 1, this limits the maximum power-split ratio for a conventional hybrid-ring coupler to approximately 9 dB.

To obtain a higher power-split ratio between the output ports, the three-quarter wavelength line in the ring is split into three quarter-wavelength lines of characteristic admittances Y_1 and Y_2, as illustrated in Figure 2. This modified

Table 1. Characteristic impedances of the lines for two hybrid-ring directional couplers.

POWER-SPLIT RATIO (dB)	CONVENTIONAL HYBRID RING		MODIFIED HYBRID RING	
	Z_1	Z_2	Z_1	Z_2
0.000	70.700	70.700	70.700	70.700
1.000	66.975	75.149	68.150	73.500
2.000	63.854	80.388	65.900	76.500
3.000	61.261	86.534	63.900	79.700
4.000	59.121	93.700	62.100	83.000
5.000	57.363	102.008	60.550	86.600
6.000	55.928	111.592	59.150	90.300
7.000	54.761	122.596	57.950	94.300
8.000	53.817	135.181	56.900	98.600
9.000	53.054	149.527	55.960	103.100
10.000	52.440	165.831	55.150	107.900
11.000	51.948	184.318	54.450	113.000
12.000	51.553	205.237	53.800	118.400
13.000	51.238	228.870	53.300	124.200
14.000	50.986	255.533	52.800	130.300
15.000	50.784	285.582	52.450	137.000

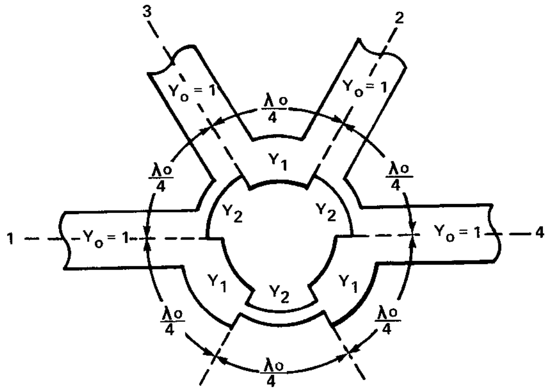

Fig. 2 Modified hybrid-ring directional coupler.

hybrid-ring directional coupler was analyzed using the scattering matrix for the four port devices. Experimental results for a stripline coupler with a power-split ratio of 7.3 dB are presented in this paper.

The modified hybrid ring is similar to the conventional hybrid ring in that (a) its input impedance is matched when the two output arms are terminated by matched loads, and (b) the voltages in the two output arms are either in-phase or 180° out-of-phase, depending on the input arms chosen. The power-split ratio is adjusted by varying the impedances of the lines in the ring between the arms.

The modified hybrid ring coupler differs from the conventional ring coupler in that (a) power-split ratios between the output ports depend on the input arms chosen, and (b) the two output arms are not perfectly isolated at the center frequency, but provide sufficient isolation to satisfy requirements for most applications.

ANALYSIS OF THE HYBRID-RING DIRECTIONAL COUPLER

The configuration of the modified hybrid-ring directional coupler is illustrated in Figure 2. The characteristic admittances of the four arms are equal and normalized to unity. The variable parameters are the two characteristic admittances Y_1 and Y_2 of the quarter-wave lines of the ring; these two admittances determine the power-split ratio between the two output arms and the impedance matching condition for the input arm.

The modified hybrid-ring coupler was analyzed by using the procedure for the analysis of symmetrical four-port networks [1,2], and by reducing the four-port network to a two-port network by taking advantage of the symmetry about the plane A-B. When two in-phase waves of unit amplitude are applied to terminals 1 and 4 or to terminals 2 and 3, the current is zero at the plane A-B. As a result, the ring can be open-circuited at this plane, and only one half of the circuit needs to be analyzed. This condition is referred to as the even mode, and all parameters associated with this mode are denoted by subscript e (see Figure 3). Similarly, when two opposite- phase waves of unit amplitude are applied to terminals 1 and 4 or to terminals 2 and 3, the voltage is zero at the plane A-B. As a result, the ring can be short-circuited at this plane, and only one half of the circuit needs to be analyzed. This condition is referred to as the odd mode, and all parameters associated with this mode are identified by the subscript o (Figure 4). The equivalent circuits for these two modes are shown in Figures 3(d) and 4(d), respectively.

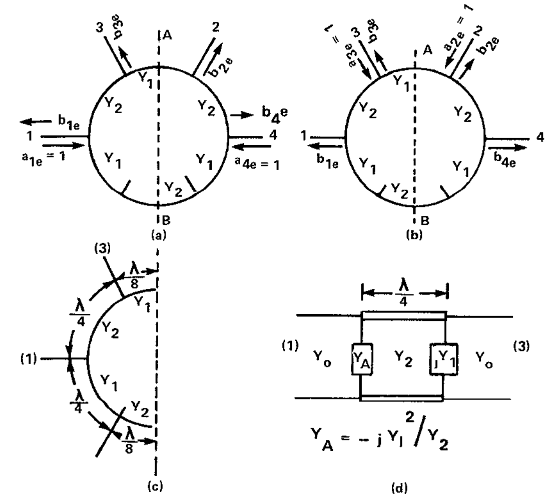

Fig. 3 Even mode. (a) Incident waves at arms 1 and 4; (b) incident waves at arms 2 and 3; (c) open circuit at A-B; (d) equivalent circuit.

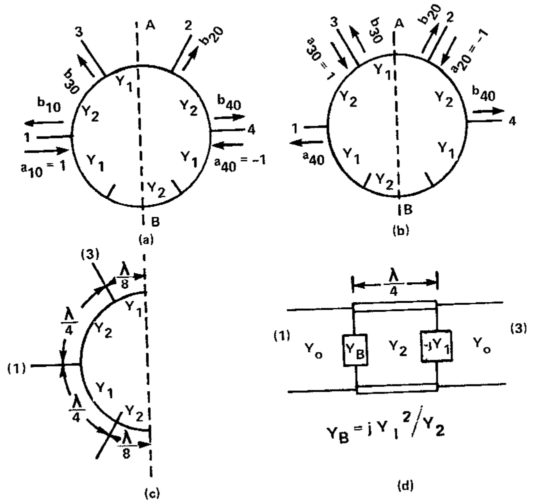

Fig. 4 Odd mode. (a) Incident waves at arms 1 and 4; (b) incident waves at arms 2 and 3; (c) short circuit at A-B; (d) equivalent circuit.

When the incident leaves are at arms 3 and 2, and the even and odd modes are superimposed, the resultant incident waves at arms 3 and 2 are given by:

$$a_3 = 2 \quad \text{and} \quad a_2 = 0 \qquad [4]$$

The output voltage ratio between arms 1 and 2 for this mode, which is referred to as the sum mode, is given by:

$$\frac{b_1}{b_2} = \frac{Y_2 \quad (1 + Y_2^2 + Y_1^3/Y_2)}{Y_1[1+Y_1/Y_2(Y_2^2 + Y_1^3/Y_2)]} \qquad [5]$$

Similarly, when the incident waves are at arms 1 and 4, and the even and odd modes are superimposed, the resultant incident waves at arms 1 and 4 are given by:

$$a_1 = 2 \quad \text{and} \quad a_4 = 0 \qquad [6]$$

The output voltage ratio between arms 3 and 4 for this mode, which is referred to as the difference mode, is given by:

$$\frac{b_3}{b_4} = - \frac{Y_2(1 + Y_2^2 + Y_1^3/Y_2)}{Y_1[Y_1/Y_2 + (Y_2^2 + Y_1^3/Y_2)]} \qquad [7]$$

In both cases, the condition that the input arm be perfectly matched requires that the reflected wave at arm 3 for the sum mode, and the reflected wave at arm 1 for the difference mode, be zero. For a given voltage ratio at the output arms, the values Y_1 and Y_2 can be calculated by solving equation [5] for the sum mode and [7] for the difference mode, while simultaneously satisfying the condition that the input port be matched. A matched power divider with any power ratio can be designed using proper admittances Y_1 and Y_2.

The characteristic impedance values Z_1 and Z_2 for various power-split ratios for the sum mode are presented in Table 1. Comparing the impedance values for the modified hybrid ring and the conventional ring, the range of attainable power-split ratios is significantly increased for the same realizable impedance values. For example, for an impedance value of 137 ohms, the coupling ratio is 15 dB for the modified ring and approximately 8 dB for the conventional ring.

The results obtained above are for a single frequency. To find the frequency dependence of this hybrid coupler, it is necessary to consider the variations in the lengths of the quarter-wave lines with the frequency in the equivalent circuits. The frequency characteristics of this hybrid-ring coupler were obtained by analyzing the circuit on MIDAS (a computer program for analyzing microwave circuits)[3]. The power-split ratio, isolation between ports, phase difference between output ports, and input VSWR for a hybrid ring with a power-split ratio of 7.3 dB are plotted in Figure 5 as a function of frequency (15 - 18 GHz), along with the experimental results discussed in the next section. From these figures, we note that the hybrid-ring coupler has a bandwidth of approximately 20 percent at Ku-band.

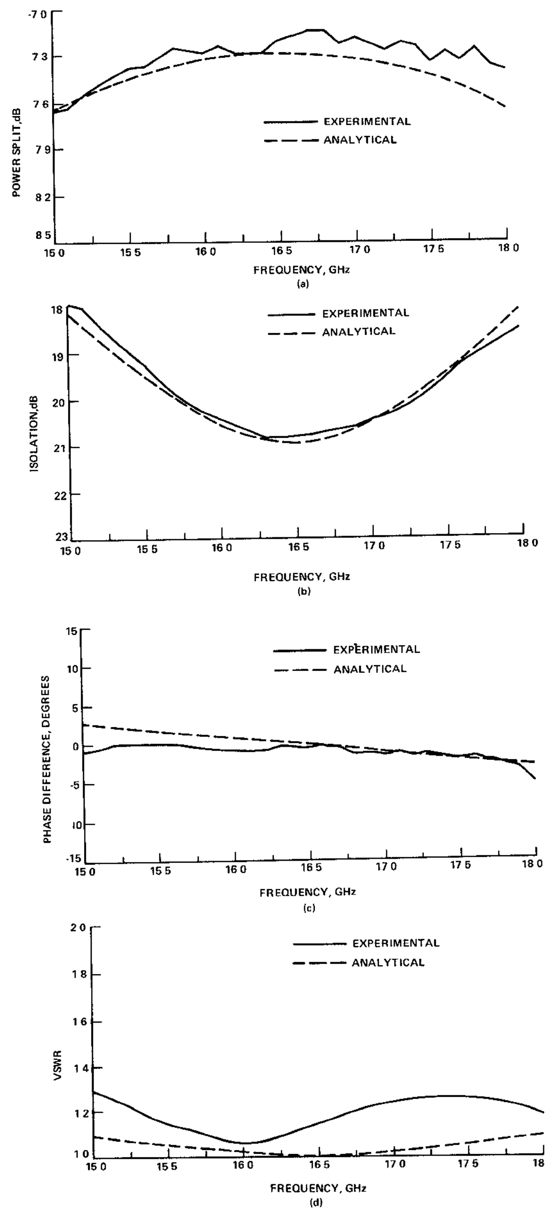

Fig. 5 Performance of the 7.3 dB hybrid-ring coupler. (a) power-split P_1/P_2; (b) isolation between ports 1 and 2; (c) phase difference between ports 1 and 2; (d) input VSWR at port 3.

EXPERIMENTAL RESULTS

A stripline hybrid-ring directional coupler with a power-split ratio of 7.3 dB between the two output arms 1 and 2 (sum mode) at the center frequency of 16.5 GHz was designed and tested. The impedance values used for this ring are $Z_1 = 57.6$ ohms and $Z_2 = 95.5$ ohms. The measured power-split ratio, isolation, the phase difference between the output ports, and input VSWR are shown in Figure 5 along with the analytical results. A close agreement between the analytical and experimental results is observed over the frequency range of 15 to 18 GHz. The input port is fairly well matched, with a VSWR of less than 1.3:1 over the frequency band.

The stripline hybrid rings were fabricated on a 50 mil Duroid 5880 substrate. Duroid 5880 substrate has a dielectric constant of 2.2 and provides low circuit loss.

CONCLUSIONS

The analysis and design of a hybrid-ring directional coupler that provides a higher power-split ratio than the conventional hybrid-ring coupler has been presented. The measured results for a coupler developed in stripline configuration at Ku-band agree well with the analytical results. The hybrid-ring directional coupler has a bandwidth of approximately 20 percent. The input arm of the coupler is matched (VSWR $<$ 1.3:1) over the frequency band. The power-split ratio can be adjusted by varying the characteristic impedances (Z_1 and Z_2) of the two lines forming the ring. Similar hybrid-ring directional couplers can also be realized in microstrip configuration.

ACKNOWLEDGMENT

The authors would like to acknowledge several helpful discussions with Mr. Farzin Lalezari of Ball Aerospace Corporation, and thank Mr. Vince Zvanya for his contributions in the fabrication of the hybrid rings.

REFERENCES

(1) C.Y. Pon, "Hybrid-Ring Directional Coupler for Arbitrary Power Division," IEEE Trans. Microwave Theory Tech., Vol. MTT-9, pp. 529-535: Nov. 1961.

(2) J. Reed and G. J. Wheeler, "A Method of Analysis of Symmetrical Four-Port Networks," IEEE Trans. Microwave Theory Tech., Vol. MTT-4, pp. 246-252: Oct. 1956.

(3) D. Rhodes and S. Perlow, "'MIDAS' A New Microwave/RF CAD Program," 1985 International Symposium on Microwave Theory and Techniques Digest, pp. 707-710.